Bioorganic Chemistry 100 (2020) 103912

Contents lists available at ScienceDirect

Bioorganic Chemistry

journal homepage: www.elsevier.com/locate/bioorg

6-Acetyl-5-hydroxy-4,7-dimethylcoumarin derivatives: Design, synthesis, modeling studies, 5-HT_{1A}, 5-HT_{2A} and D_2 receptors affinity

Kinga Ostrowska[a,*], Anna Leśniak[d], Urszula Karczyńska[a], Paulina Jeleniewicz[a], Monika Głuch-Lutwin[b], Barbara Mordyl[b], Agata Siwek[b], Bartosz Trzaskowski[c], Mariusz Sacharczuk[d,e], Magdalena Bujalska-Zadrożny[d]

[a] Department of Organic Chemistry, Faculty of Pharmacy, Medical University of Warsaw, 1 Banacha Str., 02 097 Warsaw, Poland
[b] Department of Pharmacobiology, Faculty of Pharmacy, Jagiellonian University Medical College, 1 Medyczna Str., 30 688 Kraków, Poland
[c] Centre of New Technologies, University of Warsaw, 2C Banacha Str., 02-097 Warszawa, Poland
[d] Department of Pharmacodynamics, Faculty of Pharmacy, Centre for Preclinical Research and Technology, Medical University of Warsaw, 1 Banacha Str., 02-097 Warsaw, Poland
[e] Department of Genomics, Institute of Genetics and Animal Breeding, Polish Academy of Sciences, 36A Postepu Str., 05-552 Magdalenka, Jastrzebiec, Poland

ARTICLE INFO

Keywords:
Molecular docking
Microwave-assisted synthesis
Hydroxycoumarin derivatives
5-HT_{1A}, 5-HT_{2A}, D_2 receptor ligands
CNS activity
TST tests

ABSTRACT

Molecular docking studies using appropriate 5-HT_{1A}, 5-HT_{2A} and D_2 receptors models were used to design sixteen new 5-hydroxycoumarin derivatives with piperazine moiety (**3**–**18**). The microwave radiation have been used to synthesize them and their structures have been confirmed using mass spectrometry, ^{1}H and ^{13}C NMR. All newly prepared derivatives were evaluated for their 5-HT_{1A}, 5-HT_{2A} and D_2 receptor affinity. Seven of the synthesized derivatives showed very high affinities to 5-HT_{1A} receptor (**3**–4.0 nM, **6**–4.0 nM, **7**–1.0 nM, **9**–6.0 nM, **15**–4.3 nM, **16**–1.0 nM, **18**–3.0 nM) and one of them showed high affinities to 5-HT_{2A} receptor (**16**–8.0 nM). In the case of the D_2 receptor none of the tested derivatives showed high affinity. Compounds **7** and **16** were identified as potent antagonists of the 5-HT_{1A} receptor as shown by the [35S]GTPcS binding assay but they didn't show any antidepressant effect at the single dose tested (10 mg/kg) in the tail suspension tests.

1. Introduction

Among many families of G protein-coupled receptors (GPCRs) those implicated in proper brain function and mental disorders have always garnered a lot of attention. 5-HT receptors modulate the release of many neurotransmitters and are the target of a variety of drugs, including antidepressants, antipsychotics, hallucinogens anorectics and antimigraine agents [1–4]. Dopamine receptors are also an important class of GPCR in the vertebrate central nervous system, implicated in many neurological processes and being the target of neurologic drugs [5–7]. D_2 receptor antagonism represents a key feature of antipsychotic activity that allows mitigation of the positive symptoms of schizophrenia by reducing excessive dopamine signaling in the mesolimbic pathway. Additionally, affinity at the 5-HT_{1A}, 5-HT_{2A} and 5-HT_{2C} receptors reduce side effects of dopamine depletion in the mesocortical and nigrostriatal dopamine pathways including negative symptoms of schizophrenia, motor dysfunctions and cognitive impairments [8]. Moreover, previous investigations pointed to the possibility that blockage of the 5-HT_{1A} autoreceptors accelerates the antidepressant effects of SSRI's by augmenting extracellular serotonin release in the frontal cortex and hippocampus [9–10]. A promising new 5-HT_{1A} autoreceptor antagonist, MIN-117 was entered into a phase 2 clinical trial for the treatment of major depressive disorder (MDD) and showed a more favorable tolerability profile than a classical SSRI, but was less efficacious [11–12].

N-arylpiperazine derivatives are a large class of compounds active against one or several serotonin 5-HT and dopamine receptors [13–14]. The first literature reports on the action of *N*-phenylpiperazinyl derivatives of coumarins appeared in 1998 [15]. Further research carried out over the last 20 years allowed to determine which elements of the structure of arylpiperazine derivatives of 7-hydroxycoumarin are responsible for the high affinity to serotonin 5-HT_{1A}, 5-HT_{2A} and dopamine D_2 and D_3 receptors [15–19]. In 2017, based on the results of these works, we designed a series of arylpiperazine derivatives of 7-hydroxycoumarin [20–21], which showed subnanomolar affinities to 5-HT_{1A} receptor and low nanomolar affinities to 5-HT_{2A} receptor. In all cases high affinity was obtained for compounds with a methyl group in position C-4 at the coumarin ring, and an acetyl group in position C-8.

* Corresponding author.
E-mail address: kostrowska@wum.edu.pl (K. Ostrowska).

https://doi.org/10.1016/j.bioorg.2020.103912
Received 25 October 2019; Received in revised form 6 April 2020; Accepted 2 May 2020
Available online 05 May 2020

We also found that the position of substituents on the phenyl ring on the piperazine was very important for biological activity. The chemical nature of these substituents was found to be less important, since both electron-withdrawing (chloro, bromo) and electron-donating (methoxy) moieties in the *ortho* and/or *meta* positions of the phenyl ring of piperazine gave the highest affinities. Additionally, we discovered that the alkyl chain length between coumarin and piperazine moiety, varied between three and four carbon linkers, did not significantly affect ligand affinities.

Similar results were also obtained for a series of arylpiperazine derivatives of 5-hydroxycoumarin, which we synthesized in the same year [22]. We showed that the highest, subnanomolar affinities for 5-HT_{1A} receptor were associated with the presence of the acetyl group in the C-6 position at the coumarin ring and the substituents in the 2 or 3 position in the phenyl ring of piperazine. High affinities were achieved by compounds with both the three-carbon and four-carbon alkyl chains between the coumarin and piperazine moieties. Nevertheless, the best results for 7-hydroxycoumarin derivatives were obtained for the four-carbon linker while for 5-hydroxycoumarin derivatives for the three-carbon linker.

Guided by these findings our group was encouraged to design a new series of arylpiperazinyl derivatives of 6-acetyl-5-hydroxy-4,7-dimethylcoumarin. In this study we used arylpiperazine derivatives from our previous study as a starting point for optimization of ligands against 5-HT and D_2 receptors. We have performed docking studies of 16 new coumarin derivatives to 5-HT_{1A}, 5-HT_{2A} and D_2 receptors followed by their synthesis and receptor binding assays. Additionally, functional assays and *in vivo* tests were performed for two selected derivatives (**7** and **16**) that showed high affinity to $5HT_{1A}$ receptor.

2. Results and discussion

2.1. Molecular docking studies

The results of the molecular docking calculations for the new series of hydroxycoumarin derivatives are presented in Table 1. As in our previous reports most of these derivatives show relatively high affinities to $5HT_{1A}$ receptor, but also, unlike in our former studies, similarly high affinities to $5HT_{2A}$ receptor [22].

We decided to perform a more detailed, atomic-scale analysis of the two compounds with the best predicted affinity to $5HT_{1A}$ receptor, namely **3** and **15**; these have been later confirmed to also have similarly high experimental affinities (1.0/4 nM for **3** and 2.3/4.3 nM for **15**). In both cases, and in all docked $5HT_{1A}$ ligands, the ligand is anchored in the binding site via a well-known salt-bridge between D116 and the basic nitrogen atom of the piperazine, while finding additional favorable interactions with F361, Y390 and either I385 or N392 (Fig. 1). Interestingly, the docked poses of ligands with predicted binding up to the 12 nM range are all very similar with the hydroxycoumarin derivatives interacting with the same residues, though in all cases they show two major arrangements; on with the coumarin part closer to transmembrane helices 3 and (as in the case of **3**) and with this part closer to helices 5–6 (as in the case of **15**). Overall, given the expected accuracy of the method it's difficult to choose with high confidence one or two derivatives with the highest expected affinity.

Table 1
Computational Ki values to serotonergic 5-HT_{1A} and 5-HT_{2A} and dopaminergic D_2 receptors and compounds **3–18**.

Compound	5-HT_{1A}R Ki [nM]	5-HT_{2A}R	D_2R
3	1.02	35.31	5.36
4	4.55	17.89	4.51
5	3.01	6.28	13.44
6	48.04	18.06	15.97
7	11.77	2.90	7.58
8	11.74	8.81	6.66
9	8.55	58.25	4.88
10	4.92	3.16	5.29
11	4.92	3.68	8.62
12	3.61	7.87	7.10
13	27.39	4.77	6.45
14	25.10	4.26	7.82
15	2.30	12.43	2.90
16	11.92	19.21	4.21
17	700.08	11.00	17.63
18	22.04	30.85	12.16

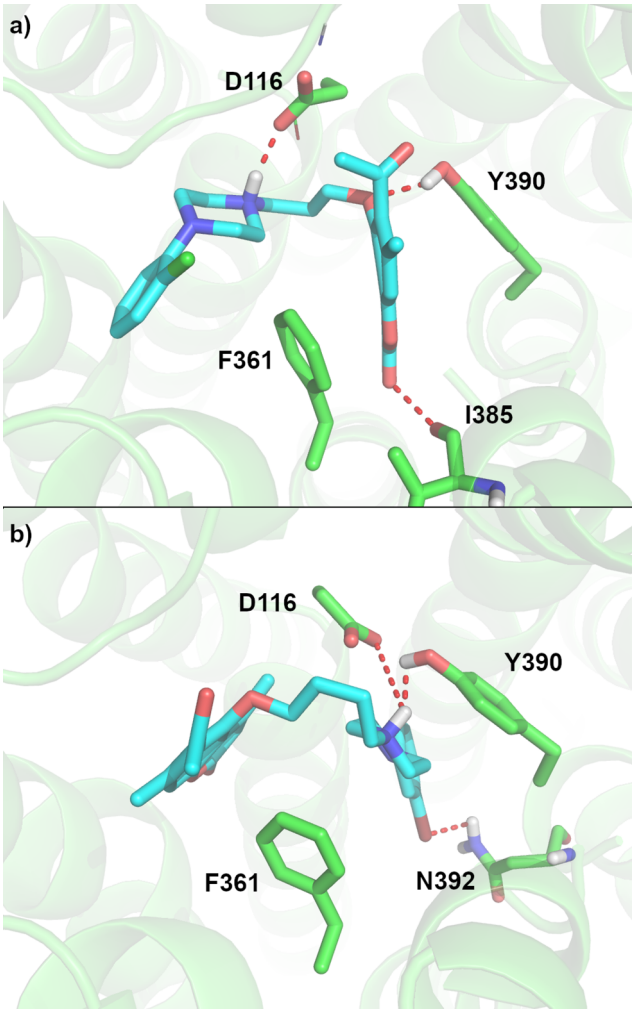

Fig. 1. Computational binding poses of (a) **3** and (b) **15** to $5HT_{1A}$ receptor.

As stated before the computational results for the $5HT_{2A}$ receptor docking are quite surprising, since in or previous studies most the coumarin derivatives active against $5HT_{2A}$ receptor had lower affinities to $5HT_{2A}$ receptor, but the agreement between the computational and experimental data was reasonably good [21,22]. Current results do not follow the trend, as the $5HT_{2A}$R computational affinity values are somewhat high, on the level of the $5HT_{1A}$R values, and clearly not in agreement with the experimental data presented in the experimental part of this study. For now we don't have an explanation for these results apart from the imperfectness of our homology $5HT_{2A}$R model which is based on the β_1 adrenergic receptor.

Additionally, we also performed computational docking studies do the D_2 receptor. Here, the results were similar to the 5 HT_{2A}R case, as most of the studies systems showed high computational affinities to D_2R, but very low experimental affinities. The high estimated computational affinities are mostly due to a strong salt bridge between D114 and the basic nitrogen atom of the piperazine, similarly to the $5HT_{1A/}$

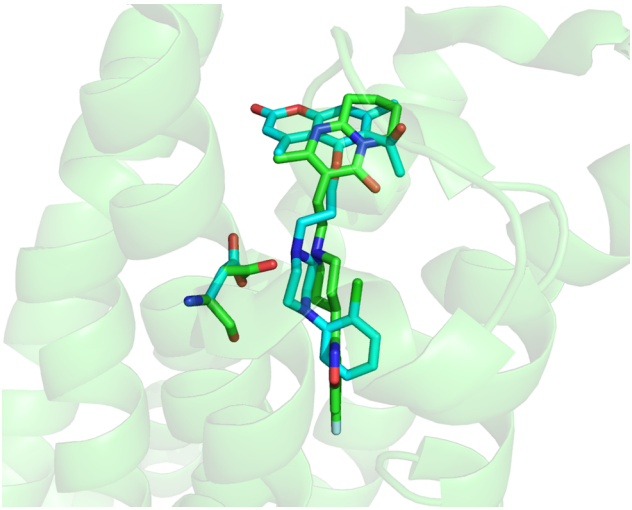

Fig. 2. Overlay of risperidone pose from the risperidone-D_2 complex crystal structure (green) and **3** pose docked to D_2 (blue) with D114 residue shown. (For interpretation of the references to colour in this figure legend, the reader is referred to the web version of this article.)

$_{2A}$R cases. This is also the same interaction that anchors the ligand in the binding pocket of the crystal structure of risperidone-D_2R complex via the salt bridge to the basic nitrogen of the piperidine moiety. Given the presence of this interaction, similar shape of risperidone and hydroxycoumarin series as well as similar poses for any studied hydroxycoumarins, which align well with the crystal structure of risperidone (Fig. 2) the final, experimental, low affinities are quite puzzling, even taking into the account the expected accuracy of the docking algorithm of around 1–2 kcal/mol.

2.2. Chemistry

A series of sixteen new arylpiperazinyl derivatives of 6-acetyl-5-hydroxy-4,7-dimethylcoumarin (**3–18**) were synthesized in two steps. First, intermediate bromoalkyl compounds (**1–2**) were prepared according to known procedures [20]. 6-Acetyl-5-(3-bromopropoxy)-4,7-dimethylcoumarin (**1**) and 6-acetyl-5-(4-bromobutoxy)-4,7-dimethylcoumarin (**2**) were prepared using microwave heating, from 6-acetyl-5-hydroxy-4,7-dimethylcoumarin and 1,3-dibromopropane or 1,4-dibromobutane as a substrates, in the presence of K_2CO_3 and KI in acetonitrile. In the next step, the final two series of new compounds (**3–10**, **11–18**) were obtained in the reaction of the suitable alkylating agent (**1** or **2**) and the corresponding *N*-substituted piperazine. Acetonitrile was used as a solvent and the reaction proceeded in the presence of potassium iodide and potassium carbonate, using a microwave reactor. The synthetic protocol is outlined in Scheme 1.

A column chromatography with appropriate solvents was used to purify new compounds. The structure of **1–18** was confirmed by appearance of two additional triplets in the range of 2.5–4.0 ppm derived from alkyl groups on the propane/butane (for 1′, 3′ or 1′, 4′ protons, respectively) and two multiplets in the range of 1.50–2.00 ppm from the remaining alkyl propane/butane groups (2′ or 2′, 3′, respectively) in ^{1}H NMR spectra. The presence of additional peaks in the aromatic range (compared to compounds **1, 2**) from the phenyl ring and signals in the range 3.50–2.50 ppm derived from the CH_2 groups in the piperazine ring, also confirmed the structures of **1–18**. In the spectra of derivatives **4–5**, **9–10**, **12–13** and **17–18**, we also observed additional signals from appropriate substituents from the piperazine phenyl ring.

2.3. In vitro affinity tests

In continuation with our efforts toward the identification of novel derivatives with serotonin 5-HT and dopamine receptors affinities, we evaluated the activity of the target systems to 5-HT_{1A}, 5-HT_{2A} and D_2 receptors using the radioligand binding assay. To determine whether the substituents in the phenyl ring have an effect on the activity, compounds with various groups attached to the phenyl ring were compared. The data (Table 2) showed that some of newly synthesized compounds possessed very high, nanomolar-range affinities to 5-HT_{1A} receptors. Among all investigated derivatives we found that those with electron-withdrawing (3-bromo, 3-fluoro) as well as electron-donating (2-methoxy) groups, (**7**, **16** and **18**, respectively) were able to bind strongly to 5-HT_{1A} receptor and showed affinities at or below the level of DPAT (K_i = 1.0 ± 0.05).. Furthermore, derivatives containing 2-chloro, 2-bromo and 2-trifluoromethyl substituents (**3**, **6**, **9**), also showed high affinity to 5-HT_{1A} receptor with the K_i values of 4.0 ± 0.4, 4.0 ± 0.5 and 6.0 ± 0.5, respectively. Clearly, the substitution at the phenyl ring is important for their activities. We also observed that for derivatives with a three-carbon linker replacing the chlorine in position C2 of the phenyl ring with bromine or a trifluoromethyl group resulted in no change or small decrease of the activity of the derivatives (compounds **3**, **6** and **9**). We also observed an over 106-fold activity loss when bromine moiety in C3 position of the phenyl ring was replaced with fluorine and 45-fold activity loss when it was replaced with two methyl groups in C3 and C5 positions (compounds **7**, **8** and **4**). For derivatives with four-carbon linker, replacing the methoxy group in C2 position with bromine, chlorine or trifluoromethyl group caused a decrease in activity, but bromine was the most preferred substituent and the trifluoromethyl group gave the derivative with the lowest affinity (compounds **18**, **14**, **11** and **17**). However, in a set of derivatives with substituents at the C3 position and the four-carbon linker, the best affinity to the 5-HT_{1A} receptor was obtained for the fluorine derivative **16**. Replacement of fluorine with bromine or methyl groups at the C3 and C5 positions caused a decrease in activity (compounds **16**, **15** and **12**).

Comparisons of compounds that differ only in the length of the alkyl chain between the coumarin and piperazinyl moiety leads to no simple structure-activity relationships. If we take into account e.g. **7** (3-carbon linker) and **15** (4-carbon linker) their affinity to 5-HT_{1A} receptor is similar but higher for **7** (K_i = 1.0 ± 0.05 for **7** or K_i = 4.3 ± 0.4 for **15**). On the other hand, for compounds **8** (3-carbon linker) and **16** (4-carbon linker) we found much better affinities for the latter compound (K_i = 106.0 ± 10.5 for **8** and K_i = 1.0 ± 0.1 for **16**). In the **10** (3-carbon linker) and **18** (4-carbon linker) pair, the derivative with the four-carbon linker had higher affinity, while in **3**/**11** and **6**/**14** pairs the derivatives with the three-carbon linker showed higher affinities (no result obtained for **10** and K_i = 3.0 ± 0.3 for **18**; K_i = 4.0 ± 0.4 for **3** and K_i = 38.0 ± 5.5 for **11**; K_i = 4.0 ± 0.5 for **6** and K_i = 17.0 ± 2.0 for **14**).

The affinity of the **3–18** series of compounds to 5-HT_{2A} receptor was also examined. Our studies have shown that new derivatives have moderate activity towards this receptor and none was active at the level of mianserin, which was used as a reference compound (K_i = 1.7 ± 0.1 for mianserin). The best results were obtained for 6-acetyl-5-(4-(4-(3-fluorophenyl)piperazin-1-yl)butoxy)-4,7-dimethyl-2H-chromen-2-one (**16**) (K_i = 8.0 ± 1.1). Its three-carbon linker analogue (**8**) had the 5-HT_{2A} receptor affinity drastically decreased (K_i > 1000). It is worth noting that compound **16**, with (3-fluorophenyl)piperazinyl moiety and four-carbon linker showed the highest affinity for both the 5-HT_{1A} and 5-HT_{2A} receptors. The remaining compounds showed affinities to 5-HT_{2A} receptor which were 1–3 orders of magnitude lower. High affinity for the 5-HT_{2A} receptors was also demonstrated by derivatives of both the three- and four-carbon linker with bromine at the C2 or C3 position of the phenyl ring on piperazine. Substitution of bromine with chlorine caused a decrease in activity, as did its conversion to a trifluoromethyl or methoxy group.

A similar situation was found in the case of the D_2 receptor affinities. As with the 5-HT_{2A} receptor, none of the tested derivatives

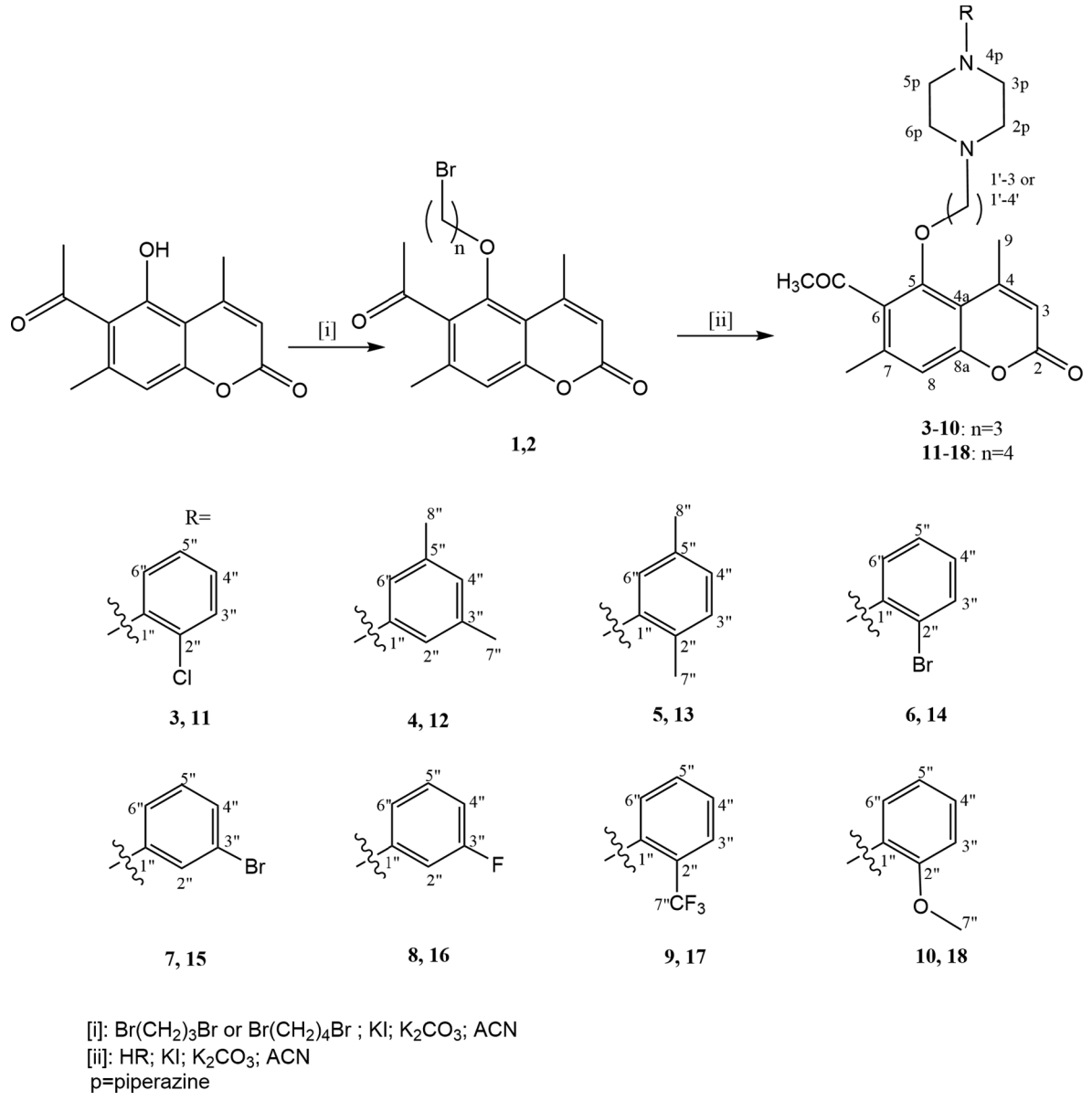

Scheme 1. Synthesis of the target compounds **3–10** and **11–18**.

showed affinities at the level of haloperidol, which was the reference compound (K_i = 2.0 ± 0.2 for haloperidol). In the case of the D_2 receptor, we obtained the highest affinities for derivatives **10** and **17**, with 2-methoxy or 2-floromethyl substituents at the phenyl ring on piperazine (K_i = 132.0 ± 6.7 for **10** and K_i = 102.0 ± 4.8 for **17**). Compound **10** had a three-carbon alkyl linker between the coumarin and piperazinyl moieties while derivative **17** had a four-carbon linker. The derivative containing the methoxy group in the C2 position was one of the most active also after changing the linker from three-carbon to four-carbon (K_i = 186.0 ± 7.0 for **18**). The remaining compounds showed much lower affinities to D_2 receptor.

2.4. Functional assays

Determination of functional activity was carried out for compounds **7** and **16** that showed the highest binding affinity at 5-HT_{1A} receptor in competition binding studies. As shown in Table 3, both **7** and **16** served as antagonists at the 5-HT_{1A} receptor. Compound **16** was more potent than **7** (IC_{50} = 537 ± 141 vs. 27 ± 2.45, p < 0.01) thus, implying that the presence of the Br atom at C3 position, together with 3-carbon linker, rather than the F atom at the same position of the aromatic determines stronger antagonist activity at the 5-HT_{1A} receptor. However, compounds **7** and **16** also exhibited moderate potency (EC_{50} = 70.5 ± 8.9 and 55.8 ± 7.3, respectively) and low efficacy (Emax = 118.7 ± 2.1 and 114.5 ± 1.7, respectively) in stimulating $G_{i/0}$ - protein activation in a 5-HT_{1A} – independent manner. This implies the engagement of an unidentified GPCR in their activity. This result is associated with receptor heterogeneity of membrane preparations from rodent tissue that is mostly not observed in transfected cell lines. It is possible that this additional partial agonist activity at this additional GPCR could have influenced the pharmacological activity of **7** and **16.**

2.5. In vivo experiments

In the TST (tail suspension test) two-way ANOVA revealed significant differences between drug-treated and control mice [($F_{4,46}$ = 3.76; p < 0.01) for **7** and ($F_{4,41}$ = 5.01; p < 0.01) for **16**]. Only the reference compound, fluoxetine (20 mg/kg, i.p) decreased immobility time, whereas compounds **7** and **16** revealed no antidepressant activity at any dose studied (1–10 mg/kg, i.p) (Fig. 3A and

Table 2
Results of binding to serotonergic 5-HT_{1A} and 5-HT_{2A} and dopaminergic D_2 receptors of references and test compounds.

Compound	5-HT_{1A}R Ki [nM] ± SEM	5-HT_{2A}R	D_2R
3	4.0 ± 0.4	85.0 ± 7.0	148.0 ± 8.8
4	45.0 ± 2.0	216.0 ± 27.0	1647.0 ± 80.2
5	80.0 ± 8.0	> 1000.0	520.0 ± 55.0
6	4.0 ± 0.5	92.0 ± 4.8	190.0 ± 9.6
7	1.0 ± 0.05	17.5 ± 1.6	580.0 ± 15.3
8	106.0 ± 10.5	> 1000.0	NO AFFINITY
9	6.0 ± 0.5	> 1000.0	647.0 ± 38.0
10	–	640.0 ± 30.5	132.0 ± 6.7
11	38.0 ± 5.5	1645.0 ± 172.0	310.0 ± 10.8
12	10.0 ± 1.5	200.0 ± 13.5	343.0 ± 30.3
13	212.0 ± 9.2	> 1000.0	557.0 ± 16.7
14	17.0 ± 2.0	90.0 ± 5.7	1285.0 ± 100.2
15	4.3 ± 0.4	55.0 ± 9.0	406.0 ± 5.4
16	1.0 ± 0.1	8.0 ± 1.1	230.0 ± 5.7
17	67.0 ± 7.0	2500.0 ± 130.0	102.0 ± 4.8
18	3.0 ± 0.3	2500.0 ± 215.0	186.0 ± 7.0
8-OH-DPAT	1.0 ± 0.05	–	–
MIANSERIN	–	1.7 ± 0.1	–
HALOPERIDOL	–	–	2.0 ± 0.2

All experiments were performed in duplicates, in three independent experiments. Data were fitted to a one-site curve-fitting equation and Ki values were estimated from the Cheng − Prusoff equation.

Table 3
Functional activity of **7** and **16** at the serotonergic 5-HT_{1A} receptor in the [^{35}S]GTPγS assay.

	Agonist mode		Antagonist mode
Compound	EC_{50} [nM ± SEM]	Emax [% ± SEM]	IC_{50} [nM ± SEM]
7	70.5 ± 8.9	118.7 ± 2.1	537 ± 141
16	55.8 ± 7.3	114.5 ± 1.7	27 ± 2.45**
8-OH-DPAT	15.3 ± 2.1	148.2 ± 7.3	n.a

Data were expressed as means ± SEM from 3 independent experiments performed in triplicate. In the agonist mode, results were normalized as percentage of response related to baseline stimulation set to 100%.
(no compound added). In the antagonist mode, results were normalized as the percentage inhibition of stimulation elicited by an EC_{80} concentration of 8-OH-DPAT (62 nM). Emax – maximum possible effect (efficacy); EC_{50} – half maximal stimulatory concentration; IC_{50} – half maximal inhibitory concentration; n.a – not applicable. Statistical significance was depicted as ** $p < 0.01$ (**7** vs. **16**, equal sum of squares F test). A single assay was performed with each compound concentrations in triplicate and the whole assay was repeated thrice.

B). The lack of any desirable antidepressant activity could have stemmed from the lack of functional selectivity for pre- and post-synaptic sites. It is possible that these compounds exert mutually exclusive biological activities upon binding to both sites. Namely, presynaptic 5-HT_{1A} autoreceptors located at somatodendritic terminals in the raphe are part of the inhibitory feedback loop and when activated, decrease serotonin release. Consequently, blockage of the presynaptic 5-HT_{1A} receptors stimulates serotonin discharge and conveys antidepressant efficacy by binding to the postsynaptic 5-HT_{1A} receptors located in various brain regions. This phenomenon was previously described in knockout mice, where suppression of 5-HT_{1A} autoreceptor expression was correlated with decreased depressive-like behavior [23]. On the other hand, blocking of the postsynaptic sites contributes to pro-depressive effects. It is also possible that 5-HT_{1A} autoreceptors show no tonic regulation of serotonin release at baseline and antagonists of these receptors only exert their antidepressant action under serotonin surge e.g following SSRI administration [24]. Moreover, the binding analysis used did not allow to determine the regional specificity of **7** and **16** at the presynaptic versus the postsynaptic 5-HT_{1A} receptors, thus their activity could heavily rely on the dose administered. This narrow therapeutic index could therefore pose difficulties in dose titration and possible large drug response variability among future patients.

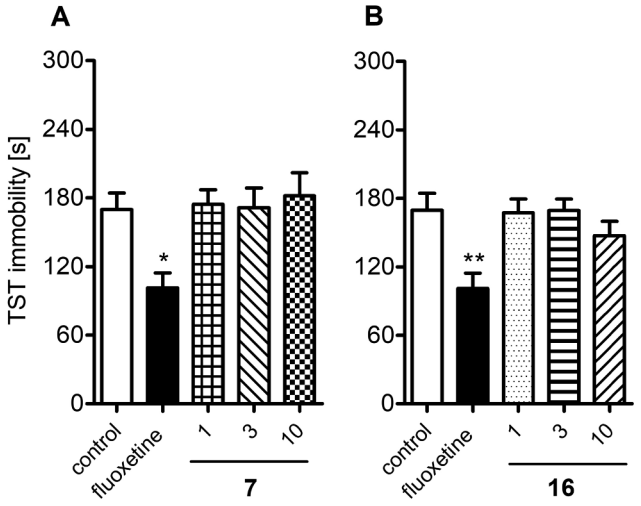

Fig. 3. Antidepressant activity of **7** (A) and **16** (B) (1–10 mg/kg, i.p.) and fluoxetine (20 mg/kg, i.p) in the tail-suspension test (TST). Asterisks represent comparisons between the treatment group and control. Two symbols represent statistical significance of $p < 0.001$ (one-way ANOVA, Bonferroni's post-hoc test, n = 8–10).

3. Conclusions

In summary, we designed and synthesized a novel series of 6-acetyl-5-hydroxy-4,7-dimethylcoumarin bearing piperazine moieties. New compounds were designed using molecular docking studies with homology models of 5-HT_{1A}, 5-HT_{2A} and D_2 receptors. Computational Ki values suggested nanomolar range of the affinity of new derivatives to 5-HT_{1A} receptors which was consistent with experimental results in receptor binding assay. Results revealed that six derivatives, both with electron-withdrawing and electron-donating group, (**3**, **6**, **7**, **9**, **15**, **16** and **18**) were able to bind strongly to 5-HT_{1A} receptor and showed affinities at or below the level of DPAT. The length of the alkyl chain between the coumarin and piperazinyl moiety had no significant effect on the affinity of the derivatives for the 5-HT_{1A} receptors. Computational affinity values for 5-HT_{2A} receptor were analogous to 5-HT_{1A} receptor and were not completely consistent with the experimental data. In this case, the calculation results were probably influenced by the application of the imperfect 5-HT_{2AR} homology model based on the β1 adrenergic receptor as well relatively large average errors connected to the docking protocol. Only compound **16** showed high affinities to 5-HT_{2A} receptors on the level of mianserin. In the case of D_2 receptors, most of the studies derivatives also showed high computational affinities, but very low experimental affinities and no derivative gave results similar to haloperidol. Finally, compounds **7** and **16** were identified as potent antagonists of the 5-HT_{1A} receptors. In the tail suspension test, however, mice injected with **7** or **16** did not decrease or prolong immobility time nor did it affect home cage activity.

4. Experimental section

4.1. Molecular docking studies

In the molecular modelling part we used models of the 5-HT_{1A} and 5-HT_{2A} receptors used in our previous studies with the same sets of flexible residues and identical parameters [20,21]. D_2 model has been prepared on the basis of the recently-solved structure of this dopamine receptor [22,25] (PDB code 6cm4). For D_2 we have used a

72 × 72 × 72 Å box centered on protein binding pocket. All other steps of docking were performed as in our previous studies [20,21]. Dopamine receptor have been treated as a rigid model with selected residues (W100, D114, F382, W386, F389, F390, Y416) of the binding pocket described in a fully flexible manner. K_i values reported in Table 2 were obtained by converting estimated ligand binding energies using the standard equation for Gibbs free energy. The expected accuracy of the docking algorithm is around 1–2 kcal/mol and while the protocol used in this investigation is generally accurate in predicting ligand poses within the binding sites of the receptors, it may be often inaccurate when it comes to estimating binding free energies; it has been shown that the latter values may err by a few orders of magnitude [27,28].

4.2. Chemistry

General: All syntheses were performed using the microwave oven, Plazmatronika 1000 W, which was equipped with a single mode niche suitable and a microwave choked outlet (30% of the power). Melting points were determined on ElectroThermal 9001 Digital Melting Point apparatus and are uncorrected. TLC was performed using Kieselgel 60 F254 sheets and spots were visualized by UV – 254 and 365 nm. Silica gel column chromatography was performer using Kieselgel 60. ^{1}H NMR and ^{13}C NMR spectra were measured at 25 °C with a Varian Unity plus-300 spectrometer. Standard Varian software was used (Varian, Inc., Palo Alto, CA, USA). High resolution mass spectra were recorded on a Quattro LCT (TOF). Reagents and solvents were used without further purification and purchased from Aldrich or Merck.

Compounds **1–2**, **3–10** and **11–18** were prepared according to the previously reported procedures [20,26].

Atom numbering, ^{1}H NMR and ^{13}C NMR spectra of all synthesized compounds is available in the ESI.

4.2.1. 6-Acetyl-5-(3-(4-(2-chlorophenyl)piperazin-1-yl)propoxy)-4,7-dimethyl-2H-chromen-2-one (3)

Yield 75%; white solid; m.p. 117–119 °C; Rf = 0.09; ^{1}H NMR (400 MHz, $CDCl_3$, δ, ppm): 7.36 (1H, d, J = 12 Hz, H-3″), 7.06 (m, 1H, H-8), 6.99 (1H, d, J = 12.8 Hz, H-6″), 6.94 (2H, m, H-4″, H-5″), 6.18 (1H, s, H-3), 3.91 (2H, t, J = 9 Hz, H-1′), 3.09 (4H, br. s, H-3p, H-5p), 2.62 (6H, m, H-2p, H-6p, H-2′), 2.57 (3H, s, H-12), 2.29 (3H, s, H-10), 2.17 (3H, s, H-9), 1.98 (2H, m, H-3′); ^{13}C NMR (75 MHz, $CDCl_3$, δ, ppm): 204.6 (C-11), 160.2 (C-2), 154.8 (C-8a), 154.5 (C-4), 152.3 (C-5), 149.4 (C-1″), 139.4 (C-7), 133.7 (C-3″), 130.8 (C-2″), 128.9 (C-5″), 127.8 (C-4″), 123.9 (C-6″), 120.5 (C-6), 116.1 (C-3), 115.3 (C-8), 112.7 (C-4a), 77.4 (C-1′), 54.6 (C-3′), 53.5 (C-3p, C-5p), 51.4 (C-2p, C-6p), 32.7 (C-12), 27.3 (C-2′), 22.7 (C-10), 19.5 (C-9); TOF MS ES+: $[M+NaCl]^+$ calcd for $C_{26}H_{29}O_4N_2NaCl$ (491.1714) found 491.1702.

4.2.2. 6-Acetyl-5-(3-(4-(3,5-dimethylphenyl)piperazin-1-yl)propoxy)-4,7-dimethyl-2H-chromen-2-one (4)

Yield 52%; white solid; m.p. 136–138 °C; Rf = 0.24; ^{1}H NMR (400 MHz, $CDCl_3$, δ, ppm): 6.97 (s, 1H, H-8), 6.54 (3H, m, H-2″, H-4″, H-6″), 6.17 (1H, s, H-3), 3.90 (2H, t, J = 8.8 Hz, H-1′), 3.18 (4H, t, J = 4.8 Hz, H-3p, H-5p), 2.58 (12H, m, H-2p, H-6p, H-9, H-10, H-2′), 2.29 (9H, m, H-12, H-7″, H-8″), 1.95 (2H, m, H-3′); ^{13}C NMR (75 MHz, $CDCl_3$, δ, ppm): 204.5 (C-11), 160.2 (C-2), 154.8 (C-5), 154.5 (C-4), 152.3 (C-8a), 151.6 (C-1″), 138.8 (C-7), 133.7 (C-3″, C-5″), 121.9 (C-4″), 116.1 (C-6), 115.3 (C-3), 114.2 (C-2″, C-6″), 112.7 (C-4a, C-8), 76.7 (C-1′), 54.6 (C-3′), 53.4 (C-3p, C-5p), 49.5 (C-2p, C-6p), 32.7 (C-12), 27.3 (C-2′), 22.7 (C-10), 21.8 (C-9), 19.5 (C-7″, C-8″); TOF MS ES+: $[M+H]^+$ calcd for $C_{28}H_{35}O_4N_2$ (463.2597) found 463.2605.

4.2.3. 6-Acetyl-5-(3-(4-(2,5-dimethylphenyl)piperazin-1-yl)propoxy)-4,7-dimethyl-2H-chromen-2-one (5)

Yield 84%; white solid; m.p. 122–124 °C; Rf = 0.20; ^{1}H NMR (400 MHz, $CDCl_3$, δ, ppm): 7.06 (1H, d, J = 10 Hz, H-3″), 6.98 (1H, s, H-8), 6.81 (2H, m, H-4″, H-6″), 6.19 (1H, s, H-3), 3.91 (2H, t, J = 8.8 Hz, H-1′), 2.94 (4H, t, J = 6.2 Hz, H-3p, H-5p), 2.63 (9H, m, H-2p, H-6p, H-12, H-2′), 2.57 (3H, s, H-10), 2.30 (6H, s, H-7″, H-8″), 2.26 (3H, s, H-9), 1.99 (2H, m, H-3′); ^{13}C NMR (75 MHz, $CDCl_3$, δ, ppm): 204.5 (C-11), 160.2 (C-2), 154.8 (C-5), 154.5 (C-4), 152.3 (C-8a), 151.4 (C-1″), 139.4 (C-7), 136.3 (C-5″), 133.7 (H-3″), 131.1 (C-2″), 129.4 (C-4″), 123.9 (C-6), 119.9 (C-6″), 116.1 (C-3), 112.7 (C-4a), 76.8 (C-1′), 54.7 (C-3′), 53.9 (C-3p, C-5p), 51.8 (C-2p, C-6p), 32.7 (C-12), 27.4 (C-2′), 22.7 (C-10), 21.4 (C-9), 19.5 (C-7″), 17.6 (C-8″); TOF MS ES+: $[M+H]^+$ calcd for $C_{28}H_{35}O_4N_2$ (463.2597) found 463.2609.

4.2.4. 6-Acetyl-5-(3-(4-(2-bromophenyl)piperazin-1-yl)propoxy)-4,7-dimethyl-2H-chromen-2-one (6)

Yield 78%; brown solid; m.p. 124–125 °C; Rf = 0.20; ^{1}H NMR (400 MHz, $CDCl_3$, δ, ppm): 7.55 (1H, d, J = 12.4 Hz, H-3″), 7.27 (1H, t, J = 11.2 Hz, H-5″), 7.06 (1H, d, J = 12.8 Hz, H-6″), 6.91 (2H, m, H-8, H-4″), 6.18 (1H, s, H-3), 3.91 (2H, t, J = 9 Hz, H-1′), 3.07 (4H, br. s., H-3p, H-5p), 2.64 (9H, m, H-2p, H-6p, H-12, H-3′), 2.29 (3H, s, H-10), 2.17 (3H, s, H-9), 1.99 (2H, m, H-2′); ^{13}C NMR (75 MHz, $CDCl_3$, δ, ppm): 204.5 (C-11), 160.1 (C-2), 154.8 (C-5), 154.4 (C-4), 152.3 (C-8a), 150.7 (C-1″), 139.4 (C-7), 133.9 (C-3″), 133.6 (H-4″), 128.4 (C-6″, C-5″), 124.5 (C-2″), 121.1 (C-6), 120.0 (C-3), 116.06 (C-8), 112.7 (C-4a), 76.7 (C-1′), 54.6 (C-3′), 53.5 (C-3p, C-5p), 51.8 (C-2p, C-6p), 32.6 (C-12), 27.3 (C-2′), 22.7 (C-10), 19.5 (C-9); TOF MS ES+: $[M+NaBr]^+$ calcd for $C_{26}H_{29}O_4N_2NaBr$ (535.1208) found 535.1227.

4.2.5. 6-Acetyl-5-(3-(4-(3-bromophenyl)piperazin-1-yl)propoxy)-4,7-dimethyl-2H-chromen-2-one (7)

Yield 73%; yellow solid; m.p. 126–127 °C; Rf = 0.08; ^{1}H NMR (400 MHz, $CDCl_3$, δ, ppm): 6.97 (5H, m, H-2″, H-4″, H-5″, H-6″, H-8″), 6.17 (1H, s, H-3), 3.92 (2H, t, J = 8.8 Hz, H-1′), 3.20 (4H, t, J = 6.6 Hz, H-3p, H-5p), 2.59 (9H, m, H-2p, H-6p, H-12, H-2′), 2.58 (3H, s, H-10), 2.29 (3H, s, H-9), 1.95 (2H, m, H-3′); ^{13}C NMR (75 MHz, $CDCl_3$, δ, ppm): 204.5 (C-11), 160.1 (C-2), 154.8 (C-5), 154.3 (C-4), 152.6 (C-8a), 152.2 (C-1″), 139.3 (C-7), 133.6 (C-5″), 130.4 (C-3″), 123.4 (H-4″), 122.3 (C-6), 118.8 (C-2″), 116.1 (C-6″), 115.3 (C-3), 114.5 (C-8), 112.7 (C-4a), 76.6 (C-1′), 54.2 (C-3′), 53.1 (C-3p, C-5p), 48.8 (C-2p, C-6p), 32.7 (C-12), 27.2 (C-2′), 22.7 (C-10), 19.5 (C-9); TOF MS ES+: $[M+NaBr]^+$ calcd for $C_{26}H_{29}O_4N_2NaBr$ (535.1208) found 535.1221.

4.2.6. 6-Acetyl-5-(3-(4-(3-fluorophenyl)piperazin-1-yl)propoxy)-4,7-dimethyl-2H-chromen-2-one (8)

Yield 81%; brown solid; m.p. 104–106 °C;; Rf = 0.22; ^{1}H NMR (400 MHz, $CDCl_3$, δ, ppm): 7.20 (2H, m, H-5″, H-8), 6.98 (1H, s, H-2″), 6.57 (2H, m, H-4″, H-6″), 6.18 (1H, s, H-3), 3.90 (2H, t, J = 10 Hz, H-1′), 3.23 (4H, br. s, H-3p, H-5p), 2.61 (12H, m, H-2p, H-6p, H-12, H-10, H-3′), 2.29 (3H, s, H-9), 1.99 (2H, m, H-2′); ^{13}C NMR (75 MHz, $CDCl_3$, δ, ppm): 204.5 (C-11), 165.6 (C-3″), 162.4 (C-2), 160.1 (C-6), 154.8 (C-4), 152.1 (C-8a), 139.3 (C-1″), 133.7 (C-7), 130.4 (C-5″), 116.1 (C-6), 115.4(H-3), 112.7 (C-8), 111.4 (C-4″), 106.4 (C-6″), 103.1 (C-4a), 102.8 (C-2″), 76.4 (C-1′), 54.5 (C-3′), 53.0 (C-3p, C-5p), 48.6 (C-2p, C-6p), 32.7 (C-12), 27.1 (C-2′), 22.6 (C-10), 19.5 (C-9); TOF MS ES+: $[M+Na]^+$ calcd for $C_{26}H_{29}O_4N_2$ FNa (475.2009) found 475.1998.

4.2.7. 6-Acetyl-4,7-dimethyl-5-(3-(4-(2-(trifluoromethyl)phenyl) piperazin-1-yl)propoxy)-2H-chromen-2-one (9)

Yield 74%; white solid; m.p. 117–118 °C; Rf = 0.26; ^{1}H NMR (400 MHz, $CDCl_3$, δ, ppm): 7.62 (1H, d, J = 10.4 Hz, H-3″), 7.51 (1H, t, J = 10.4 Hz, H-5″), 7.38 (1H, d, J = 10.4 Hz, H-6″), 7.22 (1H, m, H-4″), 6.98 (1H, s, H-8), 6.18 (1H, s, H-3), 3.91 (2H, t, J = 8.8 Hz, H-1′), 2.96 (4H, t, J = 6.2 Hz, H-3p, H-5p), 2.56 (12H, m, H-2p, H-6p, H-12, H-2′, H-10), 2.30 (3H, s, H-9), 1.98 (2H, m, H-3′); ^{13}C NMR (75 MHz, $CDCl_3$, δ, ppm): 204.5 (C-11), 160.2 (C-2), 154.8 (C-5), 154.5 (C-4), 152.7 (C-8a), 152.3 (C-1″), 139.4 (C-7), 133.7 (C-5″), 132.9 (C-3″), 127.4 (H-7″), 127.3 (C-4″), 127.3 (C-6), 124.9 (C-2″), 116.1 (C-6″), 115.3 (C-8), 112.7 (C-4a), 76.8 (C-1′), 54.7 (C-3′), 53.7 (C-3p, C-5p), 53.6 (C-2p, C-6p), 32.7 (C-12), 27.3 (C-2′), 22.7 (C-10), 19.5 (C-9); TOF

MS ES+: $[M+H]^+$ calcd for $C_{27}H_{30}O_4N_2F_3$ (503.2161) found 503.2158.

*4.2.8. 6-Acetyl-5-(3-(4-(2-methoxyphenyl)piperazin-1-yl)propoxy)-4,7-dimethyl-2H-chromen-2-one (**10**).*

Yield 75%; white solid; m.p. 122–124 °C; Rf = 0.33; ^{1}H NMR (400 MHz, $CDCl_3$, δ, ppm): 6.93 (5H, m, H-8, H-3″, H-4″, H-5″, H-6″), 6.17 (1H, s, H-3), 3.90 (5H, m, H-1′, H-7″), 3.10 (4H, br. s., H-3p, H-5p), 2.62 (4H, m, H-2p, H-6p), 2.55 (3H, s, H-12), 2.53 (3H, s, H-10), 2.51 (2H, m, H-2′), 2.29 (3H, s, H-9), 1.98 (2H, m, H-3′); ^{13}C NMR (75 MHz, $CDCl_3$, δ, ppm): 204.5 (C-11), 160.2 (C-2), 154.8 (C-1′), 154.5 (C-5), 152.4 (C-4), 152.3 (C-8a), 141.4 (C-7), 139.4 (C-2″), 133.6 (C-6″), 123.1 (H-4″), 121.2 (C-5″), 118.4 (C-6), 116.1 (C-3″), 115.3 (C-3), 112.7 (C-8), 111.4 (C-4a), 76.8 (C-1′), 54.5 (C-3′), 54.7 (C-3p, C-5p), 53.6 (C-7″), 50.8 (C-2p, C-6p), 32.7 (C-12), 27.4 (C-2′), 22.7 (C-10), 19.5 (C-9); TOF MS ES+: $[M+H]^+$ calcd for $C_{27}H_{33}O_5N_2$ (465.2389) found 465.2380.

*4.2.9. 6-Acetyl-5-(4-(4-(2-chlorophenyl)piperazin-1-yl)butoxy)-4,7-dimethyl-2H-chromen-2-one (**11**)*

Yield 54%; brown solid; m.p. 97–99 °C; Rf = 0.15; ^{1}H NMR (400 MHz, $CDCl_3$, δ, ppm): 7.35 (1H, d, J = 12 Hz, H-3″), 7.23 (1H, d, J = 8 Hz, H-6″), 7.05 (3H, H-8, H-4″, H-5″), 6.19 (1H, s, H-3), 3.85 (2H, t, J = 8 Hz, H-1′), 3.17 (4H, br.s, H-3p, H-5p), 2.61 (12H, m, H-2p, H-6p, H-4′, H-10, H-12), 2.30 (3H, s, H-9), 1.71 (4H, m, H-2′, H-3′); ^{13}C NMR (75 MHz, $CDCl_3$, δ, ppm): 205.1 (C-11), 160.0 (C-2), 154.8 (C-6), 153.4 (C-4), 151.7 (C-8a), 147.1 (C-1″), 138.9 (C-7), 133.8 (C-3″), 130.9 (C-2″), 128.9 (C-5″), 128.2 (C-4″), 125.6 (C-6″), 121.3 (C-6), 116.4 (C-3), 115.6 (C-8), 112.7 (C-4a), 77.6 (C-1′), 57.3 (C-3′), 52.6 (C-3p, C-5p), 48.1 (C-2p, C-6p), 33.2 (C-12), 29.2 (C-2′), 27.2 (C-3′), 22.5 (C-10), 19.3 (C-9); TOF MS ES+: $[M+H]^+$ calcd for $C_{27}H_{32}ClO_4N_2$ (482.9931) found 483.2005.

*4.2.10. 6-Acetyl-5-(4-(4-(3,5-dimethylphenyl)piperazin-1-yl)butoxy)-4,7-dimethyl-2H-chromen-2-one (**12**)*

Yield 54%; oil; Rf = 0.10; ^{1}H NMR (400 MHz, $CDCl_3$, δ, ppm): 6.99 (1H, s, H-8) 6.76 (2H, s, H-2″, H-6″), 6.54 (1H, s, H-4″), 6.19 (1H, s, H-3), 3.85 (2H, t, J = 9 Hz, H-1′), 3.20 (4H, m, H-3p, H-5p), 2.59 (9H, m, H-9, H-10, H-12), 2.46 (4H, m, H-2p, H-6p), 2.31 (2H, m, H-4′), 2.29 (6H, s, H-7″, H-8″), 2.18 (2H, m, H-2′), 1.81 (2H, m, H-3′); ^{13}C NMR (75 MHz, $CDCl_3$, δ, ppm): 204.6 (C-11), 160.2 (C-2), 154.9 (C-5), 154.3 (C-4), 151.6 (C-8a), 143.2 (C-1″), 139.4 (C-7), 133.6 (C-5″, C-3″), 124.2 (C-4″), 116.1 (H-2″, C-C6″), 113.6 (C-3), 110.3 (C-8), 108.0(C-4a), 78.4 (C-1′), 58.3 (C-4′), 53.5 (C-3p, C-5p), 49.5 (C-2p, C-6p), 32.7 (C-12), 27.4 (C-2′), 24.3 (C-3′), 23.8 (C-3″), 23.3 (C-10), 22.2 (C-9), 21.5 (C7″, C-8″); TOF MS ES+: $[M+Na]^+$ calcd for $C_{29}H_{36}O_4N_2Na$ (499.2573) found 499.2584.

*4.2.11. 6-Acetyl-5-(4-(4-(2,5-dimethylphenyl)piperazin-1-yl)butoxy)-4,7-dimethyl-2H-chromen-2-one (**13**)*

Yield 56%; brown solid; m.p. 113–115 °C; Rf = 0.20; ^{1}H NMR (400 MHz, $CDCl_3$, δ, ppm): 7.06 (1H, d, J = 10 Hz, H-3″) 6.98 (1H, s, H-8), 6.81 (2H, m, H-4″, H-6″), 6.18 (1H, s, H-3), 3.84 (2H, t, J = 9 Hz, H-1′), 2.93 (4H, t, J = 6 Hz, H-3p, H-5p), 2.58 (6H, m, H-2p, H-6p, H-4′), 2.56 (3H, s, H-10), 2.30 (6H, m, H-9, H-12), 2.25 (3H, s, H-8″), 2.17 (3H, s, H-7″), 1.83 (2H, m, H-2′), 1.61 (2H, m, H-3′); ^{13}C NMR (75 MHz, $CDCl_3$, δ, ppm): not registered; TOF MS ES+: $[M+Na]^+$ calcd for $C_{29}H_{36}O_4N_2Na$ (499.2573) found 499.2584.

*4.2.12. 6-Acetyl-5-(4-(4-(2-bromophenyl)piperazin-1-yl)butoxy)-4,7-dimethyl-2H-chromen-2-one (**14**)*

Yield 61%; oil; Rf = 0.35; ^{1}H NMR (400 MHz, $CDCl_3$, δ, ppm): 7.02 (4H, m, H-3″, H-4″, H-5″, H-8), 6.82 (1H, d, J = 13.2 Hz, H-6″), 6.17 (1H, s, H-3), 3.83 (2H, t, J = 9 Hz, H-1′), 3.19 (4H, t, J = 6.6 Hz, H-3p, H-5p), 2.57 (7H, m, H-2p, H-6p, H-12), 2.24 (2H, m, H-4′), 2.28 (3H, s, H-10), 2.16 (3H, s, H-9), 1.81 (2H, m, H-2′), 1.65 (2H, m, H-3′); ^{13}C NMR (75 MHz, $CDCl_3$, δ, ppm): 204.6 (C-11), 160.1 (C-2), 158.9 (C-5), 157.9 (C-4), 154.4 (C-8a), 152.3(C-1″), 139.4 (C-7), 133.6 (C-3″), 130.5 (C-4″), 124.9 (C-5″), 123.4 (C-6″), 122.3 (C-2″), 118.7 (C-6), 116.1 (C-3), 115.4 (C-8), 114.4 (C-4a), 78.4 (C-1′), 62.6 (C-4′), 58.0 (C-3p), 53.2 (C-5p), 48.8 (C-2p), 44.8 (C-6p), 32.8 (C-12), 27.9 (C-2′), 23.3 (C-3′), 21.3 (C-10), 19.5 (C-9); TOF MS ES+: $[M+H]^+$ calcd for $C_{27}H_{32}O_4N_2Br$ (527.1545) found 527.1554.

*4.2.13. 6-Acetyl-5-(4-(4-(3-bromophenyl)piperazin-1-yl)butoxy)-4,7-dimethyl-2H-chromen-2-one (**15**)*

Yield 62%; oil; Rf = 0.29; ^{1}H NMR (400 MHz, $CDCl_3$, δ, ppm): 7.03 (5H, m, H-2″, H-4″, H-5″, H-6″, H-8), 6.17 (1H, s, H-3), 3.83 (2H, t, J = 9 Hz, H-1′), 3.20 (4H, t, J = 6.6 Hz, H-3p, H-5p), 2.58 (7H, m, H-2p, H-6p, H-12), 2.24 (2H, m, H-4′), 2.29 (3H, s, H-10), 2.17 (3H, s, H-9), 1.82 (2H, m, H-2′), 1.63 (2H, m, H-3′); ^{13}C NMR (75 MHz, $CDCl_3$, δ, ppm): 204.4 (C-11), 157.9 (C-2), 157.4 (C-5), 154.4 (C-4), 150.2 (C-8a, C-1″), 143.2 (C-7), 131.0 (C-5″), 124.8 (C-3″), 123.5 (C-4″), 122.4 (C-5), 119.6 (C-2″), 118.8 (C-6″), 115.4 (C-3), 113.6 (C-8), 110.3 (C-4a), 69.0 (C-1′), 62.6 (C-5p), 59.4 (C-3p), 53.2 (C-4′), 48.8 (C-6p), 44.8 (C-2p), 32.5 (C-12), 27.4 (C-2′), 24.3 (C-3′), 23.8 (C-10), 21.6 (C-9); TOF MS ES+: $[M+Na]^+$ calcd for $C_{27}H_{31}O_4N_2NaBr$ (549.1365) found 549.1371.

*4.2.14. 6-Acetyl-5-(4-(4-(3-fluorophenyl)piperazin-1-yl)butoxy)-4,7-dimethyl-2H-chromen-2-one (**16**)*

Yield 67%; oil; Rf = 0.23; ^{1}H NMR (400 MHz, $CDCl_3$, δ, ppm): 7.20 (1H, m, H-5″), 6.97 (1H, s, H-8), 6.61 (3H, m, H-2″, H-4″, H-6″), 6.18 (1H, s, H-3), 3.84 (2H, t, J = 8 Hz, H-1′), 3.21 (4H, t, J = 8 Hz, H-3p, H-5p), 2.60 (7H, m, H-2p, H-6p, H-12), 2.55 (3H, s, H-10), 2.43 (2H, m, H-4′), 2.29 (3H, s, H-9), 1.83 (2H, m, H-2′), 1.64 (2H, m, H-3′); ^{13}C NMR (75 MHz, $CDCl_3$, δ, ppm): 204.6 (C-11), 165.6 (C-3″), 162.4 (C-2), 160.2 (C-5), 154.8 (C-4), 153.1 (C-8a), 139.4 (C-1″), 133.6 (C-7), 130.3 (C-5″), 116.1 (C-6), 112.7 (C-3), 11.2 (C-8), 108.5 (C-4″), 105.8 (C-6″), 104.1 (C-4a), 102.6 (C-2″), 78.4 (C-1′), 62.6 (C-4′), 58.0 (C-5p), 53.2 (C-3p), 48.8 (C-6p), 44.8 (C-2p), 32.7 (C-12), 27.9 (C-2′), 22.7 (C-3′), 21.6 (C-10), 19.5 (C-9); TOF MS ES+: $[M+H]^+$ calcd for $C_{27}H_{32}O_4N_2F$ (467.2346) found 467.2335.

*4.2.15. 6-Acetyl-4,7-dimethyl-5-(4-(4-(2-(trifluoromethyl)phenyl) piperazin-1-yl)butoxy)-2H-chromen-2-one (**17**)*

Yield 68%; oil; Rf = 0.25; ^{1}H NMR (400 MHz, $CDCl_3$, δ, ppm): 7.62 (1H, d, J = 10.4 Hz, H-3″), 7.51 (1H, t, J = 10.2 Hz, H-5″), 7.37 (1H, d, J = 10.4 Hz, H-6″), 7.22 (1H, m, H-4″), 6.97 (1H, s, H-8), 6.18 (1H, s, H-3), 4.07 (2H, t, J = 8.4 Hz, H-1′), 3.84 (2H, t, J = 9 Hz, H-4′), 2.97 (4H, m, H-3p, H-5p), 2.60 (7H, m, H-2p, H-6p, H-12), 2.29 (3H, s, H-10), 2.17 (3H, s, H-9), 1.79 (4H, m, H-2′, H-3′); ^{13}C NMR (75 MHz, $CDCl_3$, δ, ppm): 204.6 (C-11), 161.2 (C-2), 157.5 (C-5), 154.3 (C-4), 152.4 (C-8a), 149.0 (C-1″), 143.2 (C-7), 132.9 (C-5″), 127.4 (C-3″), 124.9 (C-7″), 124.1 (C-4″), 116.1 (C-6), 115.3 (C-2″), 113.6 (C-3), 110.3 (C-8), 108.4 (C-6″), 108.0 (C-4a), 78.5 (C-1′), 69.0 (C-4′), 58.3 (C-3p, 5p), 53.8 (C-2p, 6p), 27.5 (C-12), 24.7 (C-2′), 24.3 (C-3′), 23.9 (C-10), 22.2 (C-9); TOF MS ES+: $[M+H]^+$ calcd for $C_{28}H_{32}O_4N_2F_3$ (517.2314) found 517.2302.

*4.2.16. 6-Acetyl-5-(4-(4-(2-methoxyphenyl)piperazin-1-yl)butoxy)-4,7-dimethyl-2H-chromen-2-one (**18**)*

Yield 71%; oil; Rf = 0.23; ^{1}H NMR (400 MHz, $CDCl_3$, δ, ppm): 6.94 (4H, m, H-3″, H-4″, H-5″, H-6″), 6.66 (1H, s, H-8), 6.04 (1H, s, H-3), 3.84 (2H, t, J = 10 Hz, H-1′), 3.11 (3H, br. s, H-7″), 2.65 (8H, m, H-2p, H-3p, H-5p, H-6p), 2.55 (6H, s, H-10, H-12), 2.45 (2H, m, H-4′), 2.29 (3H, s, H-9), 1.82 (2H, m, H-2′), 1.67 (2H, m, H-3′); ^{13}C NMR (75 MHz, $CDCl_3$, δ, ppm): 204.6 (C-11), 166.4 (C-2), 160.5 (C-1″), 158.2 (C-5), 155.8 (C-4), 152.4 (C-8a), 143.5 (C-7), 141.5 (C-2″), 125.2 (C-6″), 121.2 (C-4″), 118.3 (C-6), 116.1 (C-3″), 112.9 (C-8), 109.4 (C-4a), 78.4 (C-1′), 60.3 (C-7″), 58.2 (C-3p), 55.7 (C-5p), 53.6 (C-4′), 50.8 (C-2p), 46.0 (C-6p), 32.7 (C-12), 24.4 (C-2′), 22.8 (C-3′), 21.5 (C-10), 19.5 (C-

9); TOF MS ES+: $[M+H]^+$ calcd for $C_{28}H_{35}O_5N_2$ (479.2546) found 479.2534.

4.3. In vitro affinity tests

4.3.1. Preparation of solutions of test and reference compounds

10 mM stock solutions of tested compounds were prepared in DMSO. Serial dilutions of compounds were prepared in 96-well microplate in assay buffers using automated pipetting system epMotion 5070 (Eppendorf). Each compound was tested in 8 concentrations from 10–5 to 10–12 M (final concentration).

4.3.2. 5-HT_{1A} receptor binding assay

Radioligand binding was performed using membranes from CHO-K1 cells stably transfected with the human 5-HT_{1A} receptor (PerkinElmer). All assays were carried out in duplicates. 50 µl working solution of the tested compounds, 50 µl [^{3}H]-8-OH-DPAT (final concentration 0.4 nM) and 150 µl diluted membranes (10 µg protein per well) prepared in assay buffer (50 mM Tris, pH 7.4, 4 mM $CaCl_2$, 0.1% ascorbic acid) were transferred to polypropylene 96-well microplate using 96-wells pipetting station Rainin Liquidator (MettlerToledo). Serotonin (10 µM) was used to define nonspecific binding. Microplate was covered with a sealing tape, mixed and incubated for 60 min at 27 °C. The reaction was terminated by rapid filtration through GF/B filter mate presoaked with 0.5% polyethyleneimine for 30 min. Ten rapid washes with 200 µl 50 mM Tris buffer (4 °C, pH 7.4) were performed using automated harvester system Harvester-96 MACH III FM (Tomtec). The filter mates were dried at 37 °C in forced air fan incubator and then solid scintillator MeltiLex was melted on filter mates at 90 °C for 5 min. Radioactivity was counted in MicroBeta2 scintillation counter (PerkinElmer). Raw data (cpm) representing radioligand binding was plotted as a function of the logarithm of the final molar concentration of the test and reference compound. Non-linear regression of the normalized (percent radioligand binding compared to that observed in the absence of test or reference compound - total binding) raw data was performed in GraphPad Prism 6.0 (GraphPad Software) using the built-in three parameter logistic model describing ligand competition binding to radioligand-labeled sites. The log IC50 estimated from the data is used to obtain the Ki by applying the Cheng-Prusoff approximation. Goodness of fit was evaluated on the R2 value and absolute sum of squares. Quality of the assays was evaluated by checking Ki value for control compounds with value obtained from validation experiments.

4.3.3. 5-HT_{2A} receptor binding assay

Radioligand binding was performed using membranes from CHO-K1 cells stably transfected with the human 5-HT_{2A} receptor (PerkinElmer) according to the manufacturer's instructions. All assays were carried out in duplicates. 50 µl working solution of the tested compounds, 50 µl [^{3}H]-ketanserin (final concentration 1 nM) and 150 µl diluted membranes (5 µg protein per well) prepared in assay buffer (50 mM Tris, pH 7.4, 4 mM $CaCl_2$, 0.1% ascorbic acid) were transferred to polypropylene 96-well microplate using 96-wells pipetting station Rainin Liquidator (MettlerToledo). Mianserin (10 µM) was used to define nonspecific binding. Microplate was covered with a sealing tape, mixed and incubated for 60 min at 27 °C. The reaction was terminated by rapid filtration through GF/B filter mate presoaked with 0.5% polyethyleneimine for 30 min. Ten rapid washes with 200 µl 50 mM Tris buffer (4 °C, pH 7.4) were performed using automated harvester system Harvester-96 MACH III FM (Tomtec). The filter mates were dried at 37 °C in forced air fan incubator and then solid scintillator MeltiLex was melted on filter mates at 90 °C for 5 min. Radioactivity was counted in MicroBeta2 scintillation counter (PerkinElmer). Data were fitted to a one-site curve-fitting equation with Prism 6 (GraphPad Software) and Ki values were estimated from the Cheng − Prusoff equation.

4.3.4. D_2 receptor binding assay

Radioligand binding was performed using membranes from CHO-K1 cells stably transfected with the human D2 receptor (PerkinElmer). All assays were carried out in duplicates. 50 µl working solution of the tested compounds, 50 µl [3H]-methylspiperone (final concentration 0.4 nM) and 150 µl diluted membranes (3 µg protein per well) prepared in assay buffer (50 mM Tris, pH 7.4, 50 mM HEPES, 50 mM NaCl, 5 mM $MgCl_2$, 0.5 mM EDTA) were transferred to polypropylene 96-well microplate using 96-wells pipetting station Rainin Liquidator (MettlerToledo). Haloperidol (10 µM) was used to define nonspecific binding. Microplate was covered with a sealing tape, mixed and incubated for 60 min at 37 °C. The reaction was terminated by rapid filtration through GF/B filter mate presoaked with 0.5% polyethyleneimine for 30 min. Ten rapid washes with 200 µl 50 mM Tris buffer (4 °C, pH 7.4) were performed using automated harvester system Harvester-96 MACH III FM (Tomtec). The filter mats were dried at 37 °C in forced air fan incubator and then solid scintillator MeltiLex was melted on filter mates at 90 °C for 5 min. Radioactivity was counted in MicroBeta2 scintillation counter (PerkinElmer). Data were fitted to a one-site curve-fitting equation with Prism 6 (GraphPad Software) and Ki values were estimated from the Cheng − Prusoff equation.

4.3.5. Functional [^{35}S]GTPγS assay

The assay was performed on homogenates from rat hippocampi (20 µg/ml) according to the method described previously with some modifications [29]. In the agonist mode, increasing concentrations (10^{-10}–10^{-5} M) of **7** and **16** were incubated with 0.8 nM [^{35}S]GTPγS for 5 min. At 30 °C in 50 mM Tris-HCl, pH = 7.4 binding buffer supplemented with 1 mM EGTA, 3 mM $MgCl_2$, 100 mM NaCl and 30 µM GDP in a total volume of 250 µl. Unlabeled GTPγS was used to determine non-specific binding. In the antagonist mode, 62 nM of 8-OH-DPAT was added to wells containing each triplicate concentration of **7** and **16**. Samples were then vacuum mounted onto 96-well Unifilter® Plates (Perkin Elmer, USA) and filtered with 2 ml of wash buffer (50 mM Tris-HCl, pH = 7.4) using the FilterMate Harvester (Perkin Elmer, USA). After overnight drying at RT, 45 µl of EcoScint-20 scintillant (Perkin Elmer, USA) was added to every filter well. Filter-bound radioactivity was counted in a Trilux MicroBeta^2 counter (Perkin Elmer, USA). Data were fitted with non-linear regression and with the GraphPad Prism 5.0 software. The Cheng-Prusoff equation was used to determine efficacy (Emax), potency (EC_{50}) and half-maximal inhibitory activity (IC_{50}). Baseline activation was set to 100%.

4.3.5.1. In vivo experiments. Subjects were male, 8–12-week old BALB/c mice. Animals were housed in a room provided by the animal facility at the Institute of Genetics and Animal Breeding, Polish Academy of Sciences. Mice were kept in groups of up to 4 individuals in conventional clear cages with sawdust bedding and environmental enrichment. A 12/12 h light cycle, ambient temperature of 22 ± 2 °C and 55 ± 10% humidity were ensured. Animals had *ad libitum* access to pelleted food (Labofeed H, Kcynia, Poland) and tap water. In vivo experiments were given ethical clearance from the II Local Ethics Committee for Animal Experimentation in Warsaw (decision no. WAW2/159/2018).

Antidepressant activity was assessed in the tail suspension test [30]. Compounds (1–10 mg/kg) were dissolved in 5% Kalliphor and 15% DMSO in saline and delivered intraperitoneally (i.p) at Control mice received vehicle. Fluoxetine (20 mg/kg, i.p) served as positive control. Thirty minutes after injection, mice were suspended by the tail on a hook with adhesive tape in a wooden box painted light gray (h: 680 × w: 365 × d: 280 mm). The time the animal spent actively struggling was scored for 6 min. with the help of the EthoVision behavioural tracking system (Noldus Information Technology, The Netherlands). Drug solutions were prepared and coded by a technician that did not take part in behavioral testing. Animals were assigned to treatment conditions based on allocation of random numbers generated

by Excel. Care was also taken that animals in the same treatment group were of similar weight (± 2 g).

Statistical analysis Data were analyzed with GraphPad Prism 5.04 software for Windows (GraphPad Software, San Diego California USA, www.graphpad.com). Results were expressed as mean ± SEM from 3 independent experiments. Efficacy (E_{max}) and potency (EC_{50}) were calculated from the Cheng - Prusoff equation and expressed as means ± SEM from two separate experiments. Differences in potency and efficacy were calculated with the extra sum of squares F test. Raw data from the *in vivo* experiments were analysed with one-way ANOVA followed by the Dunnett's Multiple Comparison Test. Results were considered significant at $p < 0.05$.

Declaration of Competing Interest

The authors declare that they have no known competing financial interests or personal relationships that could have appeared to influence the work reported in this paper.

Acknowledgments

This project was supported by the National Science Centre, Poland, grant No. 2017/01/X/ST5/00360 (synthesis part).

Appendix A. Supplementary material

Supplementary data to this article can be found online at https://doi.org/10.1016/j.bioorg.2020.103912.

References

[1] D.E. Nichols, C.D. Nichols, Chem. Rev. 108 (2008) 1614–1641.
[2] M. Amidfar, L. Colic, M. Walter, Y.K. Kim, Curr. Psychiatr. Rev. 14 (2018) 239–244.
[3] A. Corvino, F. Fiorino, B. Severino, I. Saccone, F. Frecentese, E. Perissutti, P. Di Vaio, V. Santagada, G. Caliendo, E. Magli, Curr. Med. Chem. 25 (2018) 3214–3227.
[4] P. Rojas, J.L. Fiedler, Front. Cell. Neurosci. 10 (2016) 1–8.
[5] J.A. Girault, P. Greengard, Arch Neurol. 61 (2004) 641–644.
[6] J.M.L. Ribeiro, M. Filizola, Front. Cell. Neurosci. 12 (2019) 1–13.
[7] A.A. Roussakis, N.P. Lao-Kaim, P. Piccini, Paola, Curr. Neurol. Neurosci. 19 (2019) 67–73.
[8] J. Horacek, V. Bubenikova-Valesova, M. Kopecek, T. Palenicek, C. Dockery, P. Mohr, C. Hoschl, CNS Drugs 20 (2006) 389–409.
[9] S.E. Gartside, E.M. Cliford, P.J. Cowen, T. Sharp, Brit. J. Pharmacol. 127 (1999) 145–152.
[10] I. Hervás, C.M. Queiroz, A. Adell, F. Artigas, Brit. J. Pharmacol. 130 (2000) 160–166.
[11] T. Saijo, J. Maeda, T. Okauchi, J. Maeda, Y. Morio, Y. Kuwahara, M. Suzuki, N. Goto, T. Fukumura, T. Suhara, M. Higuchi, Plos One 7 (2012) 1–13.
[12] M. Davidson, C. Staner, J. Saoud, N. Noel, S. Werner, E. Luthringer, J. Reilly, R. Luthringer, Minerva Neuroscience Inc. Clinical trial number: NCT03446846.
[13] E.G. Martin, R.J. Elgin Jr., J.R. Mathiasen, C.B. Davis, J.M. Kesslick, W.J. Baldy, R.P. Shank, D.L. Di Stefano, C.L. Fedde, M.K. Scott, J. Med. Chem. 32 (1989) 1052–1056.
[14] V. Soskic, V. Sukalovic, S. Kostic-Rajacic, Mini-Rev. Med. Chem. 15 (2015) 988–1001.
[15] C. Teran, L. Santana, E. Uriarte, Y. Fall, L. Unelius, B.-R. Tolf, Bioorg. Med. Chem. Lett. 8 (1998) 3567–3570.
[16] Y. Chen, Y. Lan, S. Wang, H. Zhang, X. Xu, X. Liu, M. Yu, B.-F. Liu, G. Zhang, Eur. J. Med. Chem. 74 (2014) 427–439.
[17] Y. Chen, S. Wang, X. Xu, X. Liu, M. Yu, S. Zhao, S. Liu, Y. Qiu, T. Zhang, B.-F. Liu, J. Med. Chem. 56 (2013) 4671–4690.
[18] J.C. Gonzalez-Gomez, L. Santana, E. Uriarte, J. Brea, M. Villazon, M.I. Loza, M. De Luca, Bioorg. Med. Chem. Lett. 13 (2003) 175–178.
[19] L. Santana, E. Uriarte, Y. Fall, M. Teijeira, C. Teran, E. Garcıa-Martınez, B.-R. Tolf, Eur. J. Med. Chem. 37 (2002) 503–510.
[20] K. Ostrowska, K. Młodzikowska, M. Głuch-Lutwin, A. Grybos, A. Siwek, Eur. J. Med. Chem. 137 (2017) 108–116.
[21] K. Ostrowska, D. Grzeszczuk, M. Głuch-Lutwin, A. Grybos, A. Siwek, A. Leśniak, M. Sacharczuk, B. Trzaskowski, Bioorg. Med. Chem. 26 (2018) 527–535.
[22] K. Ostrowska, D. Grzeszczuk, M. Głuch-Lutwin, A. Gryboś, A. Siwek, Ł. Dobrzycki, B. Trzaskowski, Med. Chem. Comm. 8 (2017) 1690–1696.
[23] A. Ferrés-Coy, N. Santana, A. Castañé, R. Cortés, M.C. Carmona, M. Toth, A. Montefeltro, F. Artigas, A. Bortolozzi, Psychopharmacology (Berl). 225 (2013) 61–74.
[24] A. Bortolozzi, M. Amargós-Bosch, M. Toth, F. Artigas, A. Adell, J Neurochem. 88 (2004) 1373–1379.
[25] S. Wang, T. Che, A. Levit, B.K. Shoichet, D. Wacker, B.L. Roth, Nature 555 (2018) 269–273.
[26] K. Ostrowska, D. Grzeszczuk, D. Maciejewska, I. Młynarczuk-Biały, A. Czajkowska, A. Sztokfisz, Ł. Dobrzycki, H. Kruszewska, Monatsh. Chem. 147 (2016) 1615–1627.
[27] R.D. Malmstrom, S.J. Watowich, J. Chem. Inf. Model. 51 (2011) 1648–1655.
[28] A. Castro-Alvarez, A.M. Costa, J. Vilarrasa, Molecules 22 (2017) 136.
[29] A. Lesniak, D. Chmielewska, P. Poznanski, M. Bujalska-Zadrozny, J. Strzemecka, M. Sacharczuk, Neuroscience 404 (2019) 246–258.
[30] L. Steru, R. Chermat, B. Thierry, P. Simon, Psychopharmacology (Berl) 85 (1985) 367–370.